Computer Assisted Methods in Engineering and Science, **25**: 71–80, 2018, doi: 10.24423/cames.243

TWENTY-FIVE YEARS OF THE CAMES

Cattaneo-Vernotte bio-heat transfer equation. Identification of external heat flux and relaxation time in domain of heated skin tissue

Bohdan Mochnacki[1], Marek Paruch[2]
[1] *Technical Faculty*
University of Occupational Safety Management in Katowice
Bankowa 8, 40-007 Katowice, Poland
e-mail: bmochnacki@wszop.edu.pl
[2] *Institute of Computational Mechanics and Engineering*
Faculty of Mechanical Engineering
Silesian University of Technology
Konarskiego 18a, 44-100 Gliwice, Poland
e-mail: marek.paruch@polsl.pl

A cylindrical skin tissue domain subjected to an external heat flux is considered. Thermal processes in the domain considered are described by the Cattaneo-Vernotte equation supplemented by the appropriate boundary and initial conditions. The aim of considerations is the identification of external heat flux and relaxation time on the basis of 'measured' heating/cooling curves at the set of selected points located on the surface of the skin. The direct problem is solved using the implicit scheme of the Finite Difference Method (FDM), while at the stage of the inverse problem solution, the evolutionary algorithm is applied. In the final part of the paper the examples of computations are presented.

Keywords: bio-heat transfer, inverse problems, Cattaneo-Vernotte equation, evolutionary algorithms, finite difference method.

1. Introduction

Thermal processes occurring in domain of biological tissue can be described in the different ways. The first model was presented in 1948 by Pennes [1]. The well-known parabolic Pennes equation contains the volumetric internal heat sources connected with the perfusion and metabolism. The basic assumption leading to the adopted form of the perfusion heat source is that the tissue domain is supplied by a large number of capillary blood vessels uniformly distributed in the domain considered. The metabolic heat source is often treated as a constant value (but different for different behaviors of an individual).

Recently there has been a view that, taking into account the specific internal structure of a tissue, the hyperbolic type equations better than parabolic ones reproduce the actual course of the thermal processes taking place in the domain considered, e.g. [2–5]. In this place the Cattaneo-Vernotte equation (CVE) [6] and the dual phase lag equation can be mentioned.

The final form of the CVE results from the generalization of the Fourier law consisting in the introduction of the lag time between heat flux and temperature gradient (see: next section). In this way the effect of the finite velocity of thermal wave propagation is taken into account. The relaxation time appearing in CVE in the case of biological tissue is of the order of few to the several seconds (e.g. [7, 8]). The examples of CVE applications in the scope of bio-heat transfer can be found (among others) in [9–12].

The dual phase lag equation (DPLE) contains two lag times called 'a relaxation time' and 'a thermalization time'. This form of the energy equation is also used in the problems related to bio-heat transfer. Here, for example, the papers [13–15] may be mentioned. The basic problem when using this type of bio-heat transfer model is the selection of the right values of delay times, because in the literature the quoted quantities differ greatly among themselves.

At the stage of numerical modeling the Finite Difference Method (FDM) is applied. This method has been successfully used many times to solve the tasks based on the hyperbolic type equations, e.g. [16–18]. The authorial program concerning the direct problem solution is based on the three level implicit scheme of FDM for the objects oriented in the cylindrical co-ordinates. The system of equations associated with the transition from time t to time $t + \Delta t$ is solved using the Gaussian iteration method.

The inverse problem discussed in this paper consists of the two parameters identification, in particular the boundary condition given in the part of the upper surface of the system (the Neumann boundary condition) and the relaxation time occurring in the energy equation. The task formulated in this way is solved using the evolutionary algorithm (EA) – see: [19–23].

2. Governing equations

A start point leading to the Cattaneo-Vernotte equation is the generalized form of the Fourier law, namely

$$q(X, t + \tau_q) = -\lambda \nabla T(X, t), \tag{1}$$

where q is a heat flux, λ is a thermal conductivity, τ_q is the relaxation time, $X = \{r, z\}$ and t denote the spatial co-ordinates and time. In this way the finite velocity of thermal wave and 'delay time' of heat flux with respect to temperature gradient is taken into account.

The well-known energy equation

$$c\frac{\partial T(r,z,t)}{\partial t} = -\nabla \cdot \mathbf{q}(r,z,t), \tag{2}$$

where c is a volumetric specific heat, it can be transformed to the form of CVE when the first-order approximation of formula (1) is applied

$$\mathbf{q}(r,z,t) + \tau_q \frac{\partial \mathbf{q}(r,z,t)}{\partial t} = -\lambda \nabla T(r,z,t) \tag{3}$$

or

$$-\mathbf{q}(r,z,t) = \tau_q \frac{\partial \mathbf{q}(r,z,t)}{\partial t} + \lambda \nabla T(r,z,t). \tag{4}$$

This expression should be introduced to Eq. (2) and then

$$c\frac{\partial T(r,z,t)}{\partial t} = \tau_q \frac{\partial}{\partial t}\left[\nabla \mathbf{q}(r,z,t)\right] + \nabla\left[\lambda \nabla T(r,z,t)\right]. \tag{5}$$

Substituting $-\nabla \mathbf{q}$ by $c(\partial T/\partial t)$ one obtains

$$c\left[\frac{\partial T(r,z,t)}{\partial t} + \tau_q \frac{\partial^2 T(r,z,t)}{\partial t^2}\right] = \nabla\left[\lambda \nabla T(r,z,t)\right]. \tag{6}$$

As mentioned previously, in the case of bio-heat problems the Cattaneo-Vernotte equation contains the components connected with the perfusion and metabolism. In the presence of internal heat sources $Q(r,z,t)$ within the tissue domain Eq. (6) takes a form

$$c\left[\frac{\partial T(r,z,t)}{\partial t} + \tau_q \frac{\partial^2 T(r,z,t)}{\partial t^2}\right] = \nabla\left[\lambda \nabla T(r,z,t)\right] + Q(r,z,t) + \tau_q \frac{\partial Q(r,z,t)}{\partial t}. \tag{7}$$

Considering the axially-symmetrical task and assuming the constant value of thermal conductivity one has

$$c\left[\frac{\partial T(r,z,t)}{\partial t}+\tau_q\frac{\partial^2 T(r,z,t)}{\partial t^2}\right]=\frac{\lambda}{r}\frac{\partial}{\partial r}\left[r\frac{\partial T(r,z,t)}{\partial r}\right] + \lambda\frac{\partial^2 T(r,z,t)}{\partial z^2}+Q(r,z,t)+\tau_q\frac{\partial Q(r,z,t)}{\partial t}. \tag{8}$$

The internal heat source according to the Pennes theory [1] is a sum of two components

$$Q(r,z,t)=G_B c_B\left[T_B-T(r,z,t)\right]+Q_{\text{met}}, \tag{9}$$

where G_B [m^3 blood/m^3 tissue/s] is a perfusion coefficient, c_B is a volumetric specific heat of blood, T_B is an arterial blood temperature, Q_{met} is a metabolic heat source (treated here as a constant value). Equation (8) can be rewritten in the form

$$\left(1+\frac{\tau_q G_B c_B}{c}\right)\frac{\partial T(r,z,t)}{\partial t}+\tau_q\frac{\partial^2 T(r,z,t)}{\partial t^2}=\frac{a}{r}\frac{\partial T(r,z,t)}{\partial r} + a\frac{\partial^2 T(r,z,t)}{\partial r^2}a\frac{\partial^2 T(r,z,t)}{\partial z^2}+\frac{G_B c_B}{c}\left[T_B-T(r,z,t)\right]+\frac{Q_{\text{met}}}{c}, \tag{10}$$

where $a=\lambda/c$ is a thermal diffusivity. Equation (10) must be supplemented by the boundary and initial conditions. Thus, on the bottom of the cylinder ($z=Z$) the body core temperature T_b is given (the Dirichlet condition). On the top of the cylinder ($z=0$) the boundary condition for time less than the exposure one (t_{exp}) is non-homogeneous. For the area of external heat source action ($r\le R_0$ where R_0 is a radius of flux action) the boundary heat flux is equal to q_b. On the other part of a top surface the no-flux condition is assumed. The same condition is given on the lateral surface ($r=R$), and for $r\le R_0$ when $t>t_{exp}$. It should be pointed out, that for the Cattaneo-Vernotte equation the form of the Neumann condition is the following

$$q_b(r,z,t)+\tau_q\frac{\partial q_b(r,z,t)}{\partial t}=-\lambda\mathbf{n}\cdot\nabla T(r,z,t), \tag{11}$$

where $\mathbf{n}\cdot\nabla T(r,z,t)$ denotes a normal derivative. The initial conditions are also given

$$t=0:\quad T(r,z,0)=T_p,\qquad \left.\frac{\partial T(r,z,t)}{\partial t}\right|_{t=0}=u(r,z), \tag{12}$$

where T_p is an initial temperature, while $u(r,z)$ is a known function.

3. Numerical algorithm

Let us introduce the time grid

$$0=t^0<t^1<\ldots<t^{f-2}<t^{f-1}<t^f<\ldots<t^F<\infty \tag{13}$$

and the regular differential mesh with step h in which the five-points stars $P_{i,j}$ (central node) and $P_{i+1,j}$, $P_{i-1,j}$, $P_{i,j+1}$, $P_{i,j-1}$ (neighboring nodes). In Fig. 1 the geometrical model of the problem considered and five-point star is presented. To simplify the mathematical notation the local numeration of the nodes is introduced, in particular 0 (central node) and 1, 2, 3, 4 (neighboring nodes).

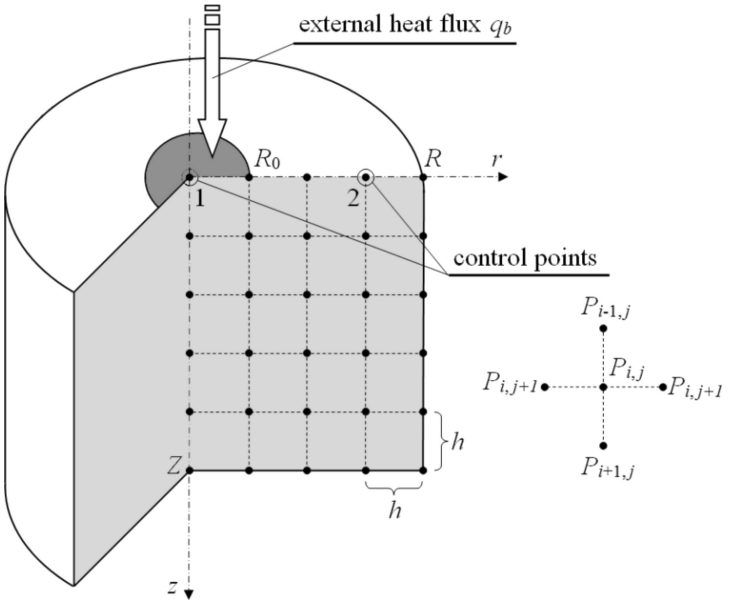

Fig. 1. The geometrical model and five-points star.

The FDM approximation of Eq. (10) for $f \geq 1$ is taken in the form

$$\left[\frac{c+\tau_q G_B c_B}{c}\right]\frac{T_0^f - T_0^{f-1}}{\Delta t} + \tau_q \frac{T_0^f - 2T_0^{f-1} + T_0^{f-1}}{\Delta t^2}$$
$$= \frac{a}{r_0}\frac{T_0^{f+1} - T_0^{f-1}}{2h} + a\frac{T_1^f + T_2^f + T_3^f + T_4^f - 4T_0^f}{h^2} + \frac{G_B c_B}{c}T_B - \frac{G_B c_B}{c}T_0^f + \frac{Q_{\text{met}}}{c} \tag{14}$$

or

$$A_0\, T_0^f - A_1\, T_1^f - A_2\, T_2^f - A_3\, T_3^f - A_4\, T_4^f = B_1\, T_0^{f-1} - B_2\, T_0^{f-2} + \frac{G_B c_B}{c}T_B + \frac{Q_{\text{met}}}{c}, \tag{15}$$

where

$$\begin{aligned}
&\frac{c+\tau_q G_B c_B}{c} = A,\\
&A_0 = \frac{A}{\Delta t} + \frac{G_B c_B}{c\Delta t} + \frac{\tau_q}{\Delta t^2} + \frac{4a}{h^2},\\
&A_1 = \frac{a}{h}\left(\frac{1}{h} + \frac{1}{2r_0}\right),\\
&A_2 = \frac{a}{h}\left(\frac{1}{h} - \frac{1}{2r_0}\right),\\
&A_3 = A_4 = \frac{a}{h^2},\\
&B_1 = \frac{A}{\Delta t} + \frac{2\tau_q}{\Delta t^2},\\
&B_2 = \frac{\tau_q}{\Delta t^2}.
\end{aligned} \tag{16}$$

In the case of the constant boundary heat flux or no-flux condition the FDM equation corresponding to formula (11) is very simple. For example, on the lateral surface $r = R$ one has

$$-\lambda\frac{T_0^f - T_1^f}{h} = 0 \quad \Rightarrow \quad T_0^f - T_1^f = 0, \tag{17}$$

etc. Assuming that for $t = 0:\ T(r,z,0) = T_p$, $u(r,z,0) = 0$ one can determine the nodal temperatures for times t^0 and t^1, namely $T_0^0 = T_0^1 = T_p$.

4. Inverse problem

The aim of investigations is to determine the relaxation time τ_q and the external heat flux q_b. The functional (fitness function) S is defined as follows

$$S(\tau_q, q_b) = \sum_{f=1}^{F}\sum_{k=1}^{K}\left(T_k^f - T_{dk}^f\right)^2 \longrightarrow \text{MIN}, \tag{18}$$

where T_k^f are the temperatures at the control points (sensors), resulting from the numerical solution of the direct problem for assumed values of τ_q and q_b, in turn T_{dk}^f are the 'postulated' or 'measured' temperatures, K is the number of sensors (here $K = 2$), F is a number of time steps. The position of the sensors is marked in Fig. 1. The minimum of functional (18) is found using the evolutionary algorithm. It is an algorithm belonging to the group of artificial intelligence methods, which does not require the analysis of the impact of design variables on the identification criterion, and allows one to obtain an optimal solution with a low risk of error. In Fig. 2 the flow chart of evolutionary algorithm is presented.

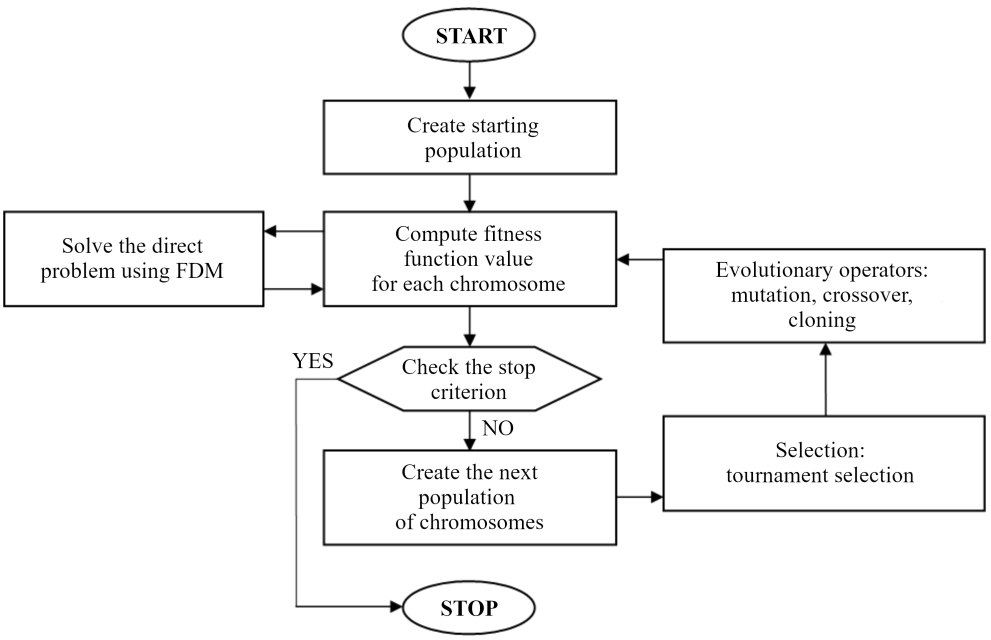

Fig. 2. Flow chart of evolutionary algorithm.

The evolutionary algorithm operates on the chromosomes population. Each chromosome contains the genes. Chromosome whose genes contain information about the identified parameters is defined in the following way

$$\mathbf{p} = \left[\ \tau_q \quad q_b\ \right]^{\mathrm{T}}, \tag{19}$$

where τ_q and q_b are the genes containing information about the relaxation time and external heat flux, respectively. The genes representing the possible solutions (parameters value) are obtained during operation of the EA, within the constraints

$$\begin{aligned} &\tau_q^L \le \tau_q \le \tau_q^H, \\ &q_b^L \le q_b \le q_b^H, \end{aligned} \tag{20}$$

where L and H denote the minimum and maximum values of the limitations imposed on the identified parameters, respectively. To solve the inverse problem, using the evolutionary algorithm, house-in software was applied. In Table 1, the parameters of evolutionary algorithm used in computations are collected.

Table 1. Evolutionary algorithm parameters.

Number of generations	Number of chromosomes	Probability of uniform mutation	Probability of nonuniform mutation	Probability of arithmetic crossover	Probability of cloning
100	50	20%	30%	50%	100%

5. Results of computations

The cylindrical domain of dimensions R = 0.03 m, Z = 0.03 m is considered. The radius of the surface on which the external heat source operates is equal to $R_0 = R/4$ (Fig. 1). Thermophysical parameters of the biological tissue are the following [4]: thermal conductivity λ = 0.5 W/(mK), volumetric specific heat of tissue c = 3 MW/(m^{3}K), blood perfusion rate G_B = 0.002 1/s, volumetric specific heat of blood c_B = 3.9962 MW/(m^{3}K), blood temperature T_B = 37°C, metabolic heat source Q_m = 245 W/m^3. The different values of relaxation time and external heat flux have been considered, the solution presented in Fig. 3 corresponds to the case 1 (see Table 2). Thus, in order to verify the correctness of an evolutionary algorithm, the identification task was solved repeatedly. The results of inverse problem solutions are collected in Table 2. It was assumed that the constraints for the identified parameters, for all cases, belong to the intervals

$$\begin{aligned} &1 \le \tau_q \le 5 \text{ s} \\ &-10000 \le q_b \le -1000 \text{ W/m}^2. \end{aligned} \tag{21}$$

Table 2. Result of computations using the EA.

Case	Design variable	Found value	Error [%]	Fitness function value (Eq. (18))
1	τ_q [s] q_b[W/m^2]	2.0818 –5004.37	4.09 0.0884	0.07895255
2	τ_q [s] q_b[W/m^2]	2.1308 –5005.27	6.54 0.1054	0.08013317
3	τ_q [s] q_b[W/m^2]	2.1241 –5012.23	6.21 0.2446	0.08522016
4	τ_q [s] q_b[W/m^2]	2.1201 –4998.94	6.01 0.0212	0.08243718
5	τ_q [s] q_b[W/m^2]	2.1018 –5005.39	5.09 0.1078	0.07896257

In Fig. 3 an example of the direct problem solution is shown, this means the temperature history in control points indicated in Fig. 1.

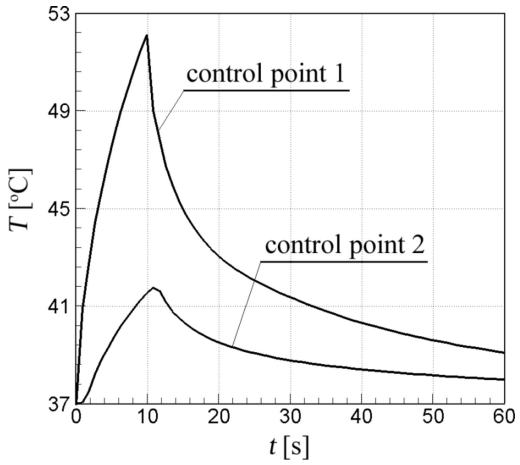

Fig. 3. The temperature history (heating/cooling curves) at the control points.

Figures 4–7 present the identification process using the evolutionary algorithm after 1st, 10th, 50th and 100th generations, respectively, for case 1 (cf. Table 2). The '◯' symbol shows the location

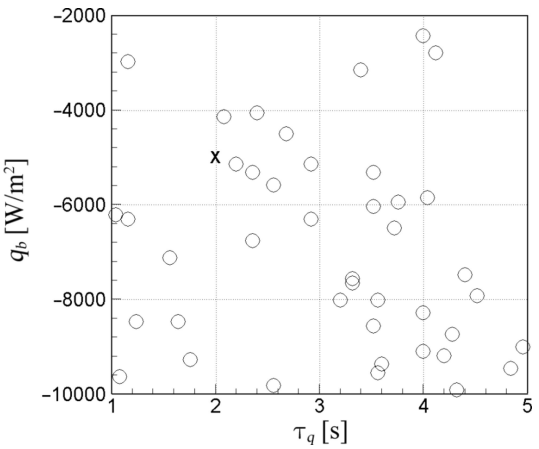

Fig. 4. The location of potential solutions after 1st generation.

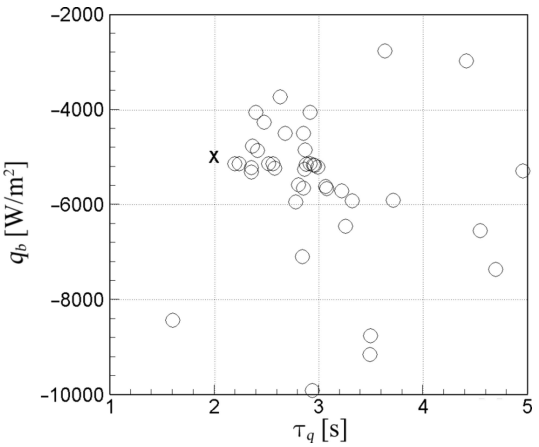

Fig. 5. The location of potential solutions after 10th generations.

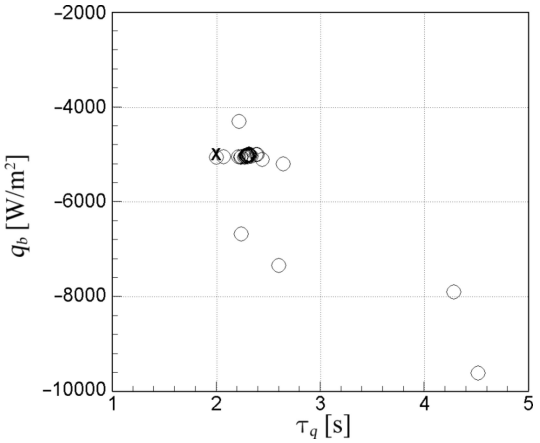

Fig. 6. The location of potential solutions after 50th generations.

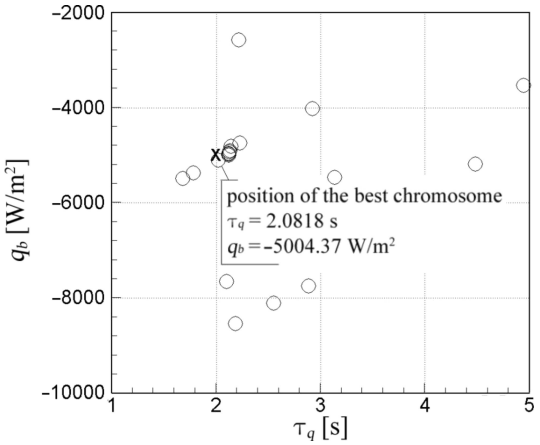

Fig. 7. The location of potential solutions after 100th generations.

of potential solutions (chromosomes) in the space of acceptable solutions (based on constraints (21)). In turn, the optimal solution for the identified parameters is indicated by the '×' symbol, i.e. τ_q = 2 s, q_b = −5000 W/m^2. Figure 8 shows the course of the fitness function for the best chromosome at each generation, obtained for the case 1 (cf. Table 2).

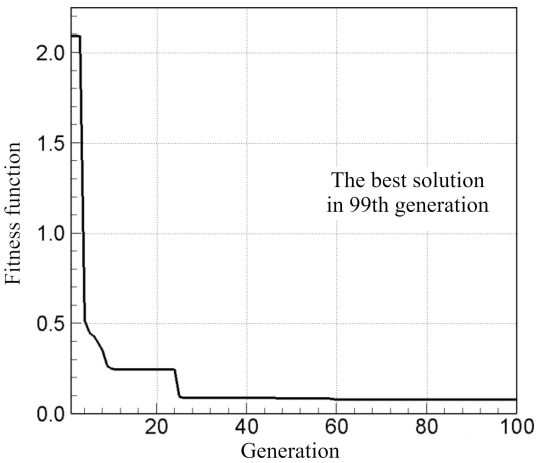

Fig. 8. Fitness function value for identification problem (case 1, Table 2).

6. Final remarks

The application of evolutionary algorithms for the solutions of identification problems is (from the numerical point of view) essentially time-consuming. The computations have been performed using the computer with a processor Intel® Core™ i7 CPU 950 @3.07 GHz with 12 GB RAM. The time necessary to carry out one identification process was equal several hours. The reduction of the identification time can be obtained by the computations parallelizing. Summing up, the solution of the inverse problem discussed in this paper is quite satisfactory. On the other hand, however, the mathematical and numerical problems connected with the adequate algorithm construction seem to be essentially simpler in comparison with the very popular gradient methods. The exactness of parameters τ_q and q_b estimation is quite satisfying.

The solutions of the direct problems have been found using the three-level implicit scheme of the FDM. The system of equations corresponding to the transition from time t to time $t + \Delta t$ has been solved iteratively (the Gauss iteration method). The additional testing calculations confirmed that the assumed spatial-time mesh is dense enough.

Acknowledgements

The paper and research are financed within the project PB3 sponsored by the University of Occupational Safety Management and the financial resources from the statutory subsidy of the Faculty of Mechanical Engineering, Silesian University of Technology in 2019.

References

[1] H.H. Pennes. Analysis of tissue and arterial blood temperatures in the resting human forearm. *Journal of Applied Physiology*, **1**: 93–122, 1948, https://doi.org/10.1152/jappl.1948.1.2.93.

[2] S. Kumar, A. Srivastava. Finite integral transform-based analytical solutions of dual phase lag bio-heat transfer equation. *Applied Mathematical Modelling*, **52**: 378–403, 2017, https://doi.org/10.1016/j.apm.2017.05.041.

[3] K.C. Liu, J.Ch. Wang. Analysis of thermal damage to laser irradiated tissue based on the dual-phase-lag model. *International Journal of Heat and Mass Transfer*, **70**: 621–628, 2014, https://doi.org/10.1016/j.ijheatmasstransfer.2013.11.044.

[4] B. Mochnacki, E. Majchrzak. Numerical model of thermal interactions between cylindrical cryoprobe and biological tissue using the dual phase lag equation. *International Journal of Heat and Mass Transfer*, **108**: 1–10, 2017, https://doi.org/10.1016/j.ijheatmasstransfer.2016.11.103.

[5] A.N. Smith, P.M. Norris. *Microscale Heat Transfer*. John Willey & Sons, New York, 2003.

[6] M.C. Cattaneo. A form of heat conduction equation which eliminates the paradox of instantaneous propagation. *Compte Rendus*, **247**: 431–433, 1958.

[7] W. Kaminski. Hyperbolic heat conduction equation for materials with a nonhomogeneous inner structure. *Journal of Heat Transfer*, **112**: 555–560, 1990, https://doi.org/10.1115/1.2910422.

[8] E. Majchrzak, L. Turchan, J. Dziatkiewicz. Modeling of skin tissue heating using the generalized dual-phase lag equation. *Archives of Mechanics*, **67**(6): 417–437, 2015.

[9] M. Ciesielski, B. Mochnacki. Hyperbolic model of thermal interactions in a system biological tissue-protective clothing subjected to an external heat source. *Numerical Heat Transfer Part A-Applications*, **74**(11): 1685–1700, 2018, https://doi.org/10.1080/10407782.2018.1541292.

[10] K. Mitra, S. Kumar, A. Vedavarz, M.K. Moallemi. Experimental evidence of hyperbolic heat conduction in processed meat. *Journal of Heat Transfer*, **117**: 568–573, 1995, https://doi.org/10.1115/1.2822615.

[11] F. Xu, K.A. Seffen, T.J. Lu. Non-Fourier analysis of skin biothermomechanics. *International Journal of Heat and Mass Transfer*, **51**: 2237–2259, 2008, https://doi.org/10.1016/j.ijheatmasstransfer.2007.10.024.

[12] M.I.A. Othman, M.G.S. Ali, M.R. Farouk. The effect of relaxation time on the heat transfer and temperature distribution in tissues. *World Journal of Mechanics*, **1**: 283–287, 2011, https://doi.org/10.4236/wjm.2011.16035.

[13] Y. Zhang. Generalized dual-phase lag bioheat equations based on non equilibrium heat transfer in living biological tissues. *International Journal of Heat and Mass Transfer*, **52**: 4829–4834, 2009, https://doi.org/10.1016/j.ijheatmasstransfer.2009.06.007.

[14] E. Majchrzak. Numerical solution of dual phase lag model of bioheat transfer using the general boundary element method. *Computer Modeling in Engineering & Sciences*, **69**(1): 43–60, 2010, https://doi.org/10.3970/cmes.2010.069.043.

[15] E. Majchrzak, B. Mochnacki. Application of numerical methods for solving the non-Fourier equations. A review of our own and collaborators' works. *Journal of Applied Mathematics and Computational Mechanics*, **17**(2): 43–50, 2018, https://doi.org/10.17512/jamcm.2018.2.04.

[16] E. Majchrzak, B. Mochnacki. Implicit scheme of the finite difference method for a second-order dual phase lag equation. *Journal of Theoretical and Applied Mechanics*, **56**: 393–402, 2018, http://dx.doi.org/10.15632/jtam-pl.56.2.393.

[17] D. Deng, Y. Jiang, D. Liang. High-order finite difference method for a second-order dual-phase-lagging models of microscale heat transfer. *Applied Mathematics and Computation*, **309**: 31–48, 2017, https://doi.org/10.1016/j.amc.2017.03.035.

[18] E. Majchrzak, B. Mochnacki. First and second order dual phase lag equation. Numerical solution using the explicit and implicit schemes of the finite difference method. *MATEC Web of Conferences*, **240**: Article Number 05018, 2018, https://doi.org/10.1051/matecconf/201824005018.

[19] B. Mochnacki, M. Paruch. Estimation of relaxation and thermalization times in microscale heat transfer. *Journal of Theoretical and Applied Mechanics*, **51**(4): 837–845, 2013.

[20] B. Mochnacki, E. Majchrzak, M. Paruch. Soft tissue freezing process. Identification of the dual phase lag model parameters using the evolutionary algorithms. *AIP Conference Proceedings*, **1922**: Article Number 060001, 2018, https://doi.org/10.1063/1.5019062.

[21] E. Majchrzak, M. Paruch. Identification of electromagnetic field parameters assuring the cancer destruction during hyperthermia treatment. *Inverse Problems in Science and Engineering*, **19**(1): 45–58, 2011, https://doi.org/10.1080/17415977.2010.531473.

[22] M. Paruch. Identification of the degree of tumor destruction on the basis of the Arrhenius integral using the evolutionary algorithm. *International Journal of Thermal Sciences*, **130**: 507–517, 2018, https://doi.org/10.1016/j.ijthermalsci.2018.05.015.

[23] Z. Michalewicz. *Genetic Algorithms + Data Structures = Evolution Programs*. Springer-Verlag, Berlin, 1996.